RSC Advances

ROYAL SOCIETY OF CHEMISTRY

www.rsc.org/advances

Journal Name ARTICLE

Encapsulation of photoactive porhyrinoids in polyelectrolyte hollow microcapsules viewed by Fluorescence Lifetime Imaging Microscopy (FLIM)

Received 00th January 20xx,
Accepted 00th January 20xx

DOI: 10.1039/x0xx00000x

www.rsc.org/

Raquel Teixeira, [*a†] Vanda Vaz Serra,[ab] Pedro M. R. Paulo,[a] Suzana M. Andrade[a] and Sílvia M. B. Costa[*a]

Fluorescence Lifetime Imaging Microscopy (FLIM) was used to investigate the encapsulation of different porphyrinoids in multilayer polyelectrolyte hollow microcapsules assembled layer by layer with poly(styrene sulfonate) (PSS) and poly(allylamine hydrochloride) (PAH). The lifetime colour contrast enables the discrimination of fluorophore interactions at the microcapsule interface or deeper localized in the microcapsule shell. The coupling of functionalized porphyrin derivatives with oppositely charged polyelectrolyte made the microcapsule pH responsive. FLIM images were also obtained from aluminium monosulphonate phthalocyanine ($AlPcS_1$) included into a lipid vesicle deposited on the surface of a modified microcapsule with dispersed gold nanoparticles (AuNP). In this case, a heterogenous distribution of both quenched and enhanced fluorescence intensities was mapped from various fluorescence spots. These effects, undetected in the absence of AuNP, were accompanied by a decrease of lifetimes attributed to the contribution of plasmonic effects induced by AuNP. Fluorescence lifetime contrast-based imaging provides new insights in the field of polyelectrolyte microcapsules.

Introduction

Hollow microcapsules (MCs) obtained from layer-by-layer (LbL) assembly of oppositely charged polyelectrolytes onto sacrificial colloidal particles arouse a great interest as they have shown potential applications in encapsulation and controlled drug release and diagnostics.[1-5] From both scientific and biotechnological viewpoints they are considered an important class of materials in catalysis conversion, food additives and, in general, for the manufacture of advanced materials.[6]

The main driving force for the preparation of synthetic microcapsules[7-8] utilizes a simple yet conventional powerful technique of polymeric electrostatic interactions in which the composition of both shell structure and core content can be monitored. The system´s design of microcapsules has a great flexibility since it provides the control of the number sequence and type of polyelectrolytes chosen. The capsules are fabricated with controlled physical and chemical properties and can provide novel structures for micro- and nano-compartmentalization of materials. In addition, unlike liposome structures[9] the fabricated shells are readily permeable by small (ca. 1 ± 2 nm in diameter) polar molecules[10] and are extremely stable against chemical and physical influences. It is envisaged that different species, with a wide diversity of chemical structures such as proteins, nucleic acids, inorganic nanoparticles or dyes can be incorporated into the shell structure creating materials with unique tailored properties which make these systems very attractive for a wide range of applications.

The most common pair of charged polyelectrolytes (PEs) are the cationic PAH poly(allylamine hydrochloride) and the anionic PSS, poly(styrene sulfonate). Hollow microcapsules obtained by LbL assembly consisting of PAH/PSS and the tetrapyrrolic dye meso-tetrakis(4-sulfonatophenyl)porphine (TPPS) incorporated in the shell wall produced a photoactive microcapsule which upon irradiation with laser light showed laser-responsive oxidative properties with the formation of active oxygen species and disruption of the capsule wall.[11] Porphyrin encapsulation, in these studies was demonstrated by confocal laser scanning microscopy (CLSM) and steady state fluorescence emission.

More detailed information on dyes encapsulation can be assessed by fluorescence lifetime imaging microscopy (FLIM) which emerged as a key technique to image the environment and interaction of specific probes in living cells. FLIM is used to discriminate different fractions of the same fluorophore in different states of interaction with its environment. Molecular effects can thus be investigated independently of the unknown and usually variable fluorophore concentration.[12]
Herein we followed the incorporation of water soluble dyes anionic meso-tetrakis(4-sulfonatophenyl) porphyrin (TSPP), cationic meso-tetrakis(N-methyl-pyridinium-4-yl) porphyrin (TMPyP) and cationic zinc meso-tetrakis(N-methyl-pyridinium

[a] *Corresponding Authors:*
raquel.teixeira@dep.uminho.pt;sbcosta@tecnico.ulisboa.pt
[b] *Centro de Química Estrutural, Instituto Superior Técnico, Universidade de Lisboa, Av. Rovisco Pais 1, 1049-001 Lisboa, Portugal*
[c] *Unidade de Química Orgânica e Produtos Naturais, Departamento de Química, Universidade de Aveiro.*
† 3Bs Research Group in Biomaterials, Biodegradables and Biomimetics, University of Minho, Headquarters of the European Institute of Excellence on Tissue Engineering and Regenerative Medicine, AvePark, 4806-909 Taipas, Guimarães, Portugal.
Electronic Supplementary Information (ESI) available: Porphyrin/Polyelectrolyte interactions ; Mechanism of TCPP-PAH synthesis; Hollow Microcapsules with Phthalocyanines; Microcapsules with Gold Nanoparticles (AuNPs) and $AlPCS_X$. See DOI: 10.1039/x0xx00000x

4-yl)porphyrin (ZnTMPyP) in PAH/PSS hollow microcapsules suspensions, using (FLIM).[13] In parallel we compared the steady-state absorption and emission as well as transient state fluorescence of the same porphyrins either in the MC shell wall or at the MC interface with the corresponding spectra in aqueous solution.

The incorporation of tetracarboxylic (TCPP) derivatives covalently linked to polyanion PAH in the microcapsules is compared with the non covalent approach employing ionic porphyrinoids. The inclusion of sparingly water-soluble π-π-vinyl pyridinium porphyrins (BOPYP) was also tested at different pHs. Also the mono-sulfonated aluminium phthalocyanine, $AlPcS_1$, which is both water-soluble and lipophilic, was incorporated in the PE MCs through the lipid bilayer coating.

The incorporation of porphyrin and phthalocyanine dyes with photo-, thermo- or electrochemical properties in the capsule shells can have potential interest for the preparation of light harvesting , remote release systems and microspheres laser approaches.[14-16] Microcapsules carrying porphyrins and phthalocyanines can also be interesting micro- or nanoreactors to perform, for instance, photocatalytic reactions. In that case, higher quantities of incorporated fluorophores could be obtained by adsorption of the molecules to several layers, which would likely improve the efficiency of photocatalysis.[17]

Experimental

Materials

Monodisperse polystyrene (PS) latex particles with a diameter of 4.06 ± 0.11 μm were purchased from Microparticles GmbH, Berlin, Germany. Poly(sodium 4-styrenesulfonate) (PSS, MW~75000, 18% wt.% in water) and poly(allylamine hydrochloride) (PAH, MW ~15000) were obtained from Sigma-Aldrich and used as received. Monosulfonated aluminium phthalocyanine ($AlPcS_1$) was synthesized according to Ambroz et al.[18] and tetrasulfonated aluminum phthalocyanine (AlPcTS, 99%) was supplied by Porphyrin Products, Frontier Scientific, Inc. Logan, Utah, USA.

Meso-tetra(4-carboxyphenyl) porphine (TCPP) was bought from Strem Chemicals Inc., Newburyport, MA, and meso-tetra(4-methylpyridyl)porphine (TMPyP) was obtained from Sigma-Aldrich. meso-tetra(4-sulfonatophenyl)porphyrin (TSPP) was obtained from Fluka (≥98% purity). Other laboratory reagents and solvents were also purchased from Sigma-Aldrich with the minimum required purity. TCPP-PAH and BOPYP were prepared respectively according to reported procedures.[19,20]

Templates' synthesis

$MnCO_3$ colloidal templates were prepared by co-precipitation of $MnSO_4$ (50 mL, 60 mM) and NH_4HCO_3 (50 mL, 0.6 M) at 40ºC and under vigorous stirring for 4 minutes. The suspension was left during 10 minutes at room temperature and then was centrifuged (4 minutes at 4000 rpm) and washed three times. $CaCO_3$ templates were also prepared by co-precipitation: equal volumes of 0.33 M solutions of $CaCl_2$ and Na_2CO_3 were rapidly mixed and thoroughly stirred for 1 min at room temperature. The reaction mixture was left without stirring for 5 minutes and then the precipitate was centrifuged and washed three times with bidistilled water.

Polyelectrolyte layer-by-layer assembly

Polyelectrolyte microcapsules were prepared by deposition of a minimum of 3 bilayers of PAH/PSS onto the colloidal particles. PAH and PSS aqueous solutions (2 mg/mL) were prepared in 0.5 M NaCl. Since all the templates used had a negative surface charge, the alternate adsorption of the oppositely charged PEs started always with the positive PAH. During each adsorption step, particles were suspended in the respective PE solution and left for 15 minutes under stirring. After deposition, the particles were centrifuged, the supernatant was removed, and the particles were dispersed in water. The centrifugation and washing with water were repeated three times before addition of the next polyelectrolyte layer.

Templates' removal

In order to obtain hollow microcapsules, the core has to be removed. This was performed after the adsorption of 3 bilayers of PAH/PSS and before the adsorption of fluorophores to assure that the microcapsules' wall has structural stability and do not disrupt after the core removal. The displacement of some fluorophore molecules along with the products of core dissolution is avoided by using this procedure.

Inorganic cores were removed by suspending the microparticles in 0.1M HCl ($MnCO_3$) or 0.2M EDTA and stirred for 30 minutes. This procedure was repeated three times and, finally, microparticles were centrifuged and washed several times with bidistilled water. In order to remove PS cores, microcapsules were dried, suspended in dimethylformamide (DMF) and left for 2h under stirring at 60ºC. This procedure was repeated once again. Microcapsules were subsequently centrifuged and washed with water.

Synthesis of porphyrin–functionalized PAH

meso-tetra(4-carboxyphenyl)porphine (TCPP, 0.1 mM), 1-ethyl-3-(3-dimethylaminopropyl)-carbodiimide (EDC; 0.1 mM) and N-hydroxysuccinimide (NHS; 0.2 mM) were mixed with PAH (2 mg/mL) in DMSO/water 1:3, at pH≈7, and left 2 hours under stirring at 60ºC. Since the PAH labelled with TCPP preserves most of its free amine functionalities and the other molecules do not adsorb to the microcapsule because they are neutral or weakly charged, the reaction mixture was used to continue the layer-by-layer assembly of microcapsules, without any purification procedure.

Adsorption of charged fluorophores

Introduction of charged fluorophores in the microcapsules was done in a single layer assembly step and simultaneously with the adsorption of the oppositely charged PE. Previously, TMPyP, ZnTMPyP or TSPP were complexed in solution with PSS or PAH (2 mg/mL), respectively, in order to obtain a final concentration of approximately 0.1 mM of dye. The hollow microcapsules with a minimum of three bilayers of PAH/PSS

were then suspended in these solutions and the adsorption/washing steps above referred to, were repeated.

Microcapsules coated with labelled DMPC lipid bilayer

The appropriate amounts of DMPC and $AlPcS_1$ were co-solubilized in 200 μL of chloroform/methanol 2:1. The solvent was evaporated under a nitrogen stream to obtain a lipid film. The film was hydrated with bidistilled water at 25-30ºC (above the main phase transition of the phospholipid (T_m=24ºC) while sonicated for 10 minutes. The final concentration of DMPC and $AlPcS_1$ was 1 mg/mL and 0.1 mM, respectively. The suspension of lipid vesicle was then centrifuged and washed in order to remove the phthalocyanine dissolved in the external water.
The lipid vesicles were mixed with a microcapsules' suspension and incubated for 20 min with stirring at a temperature above Tm to allow the lipid bilayer adsorption around the MC surface to occur. Next, the samples were centrifuged for 15 min at 4000 rpm and the supernatant was removed. Centrifugation and re-suspension with bidistilled water was repeated until no vesicles remained in the bulk.

Synthesis of gold nanoparticles (AuNPs)

Citrate-capped gold nanoparticles (AuNPs) were obtained by chemical reduction of the metal precursor salt with sodium citrate.[21] Briefly, 1.9 mL of 0.1 M sodium citrate solution was added to 48.1 mL of a boiling aqueous solution of sodium tetrachloroaurate (5×10^{-5} mol), and the mixture was left under stirring at 100ºC for 15 min. These AuNPs were used as seeds to produce larger particles through the seed-mediated growth described by Fernández et al.[22]

Steady-State Spectroscopy

Steady-state UV-visible absorption or extinction spectra were recorded either in a Jasco V-560 UV-vis spectrophotometer, with temperature control when required, or in a Perkin-Elmer Lambda 35 UV/vis spectrophotometer. Quartz cells with an optical path length of 1 cm were used, except for a few cases when reduced path length cells were needed. The necessary corrections for turbidity were carried out.[23]

Time-Resolved Fluorescence

Fluorescence decays were obtained with a HORIBA Jobin Yvon IBH FluoroLog-3 spectrofluorimeter adapted to time-correlated single photon counting (TCSPC), equipped with a Hamamatsu R928 photomultiplier tube. Samples were excited with nanosecond pulses of 445 nm generated by a NanoLED pulsed diode (Horiba). Emission decays were analyzed using the software DAS6 v6.4. Decays were fitted with reconvolution of the time-dependent profile of the light source. The best fit was assessed based on the parameter χ^2 and the distribution of the weighted residuals.

Fluorescence Lifetime Imaging Microscopy

FLIM measurements were performed with a time-resolved confocal microscope (MicroTime 200, PicoQuant GmbH). A detailed description may be found elsewhere.[13] Briefly, the excitation at 405 nm or at 639 nm is carried out by a pulsed diode laser at a repetition rate of 10/20 MHz, through a water immersion objective (60x, N.A. 1.2). Samples were placed in the microscope sample holder perpendicularly to the excitation light that propagates through the bottom of the sample. The emitted fluorescence is collected in the reverse pathway and is sent through a dichroic mirror, an emission filter (bandwidth 55 nm, centred at 695 nm), and a 50 μM pinhole that rejects out-of-focus light providing confocal detection. The fluorescence is then detected with a single-photon counting avalanche diode (SPAD) (Perkin- Elmer) whose signal is processed by TimeHarp 200 TC-SPC PCboard (PicoQuant) working in the time-tagged time-resolved (TTTR) operation mode. Each sample was imaged several times, and the fluorescence decays of more than 50 fixed points were collected from different regions of the slides.

Results and discussion

A. Polyelectrolyte/Porphyrin Interaction

Ionic porphyrins (TSPP, TMPyP and BOPYP) can react with oppositely charged polyelectrolytes. In this section are compared the absorption and fluorescence spectra in water with increasing polyelectrolyte concentrations.

a) *meso*-Tetra(4-sulfonatophenyl)porphyrin, TSPP/PAH

TSPP spectral features do not change significantly when it is mixed with the same charged PE, PSS. On the other hand, the interaction of TSPP with PAH results in the formation of H-dimers or aggregates,[24] as shown by the blue-shifted Soret peak at 401 nm in the respective absorption spectrum (Fig. S1). It is likely that the positive amine groups of PAH might induce the aggregation of TSPP and for this reason the emission is quenched, by comparison with the emission in aqueous solution. This effect has also been observed with other positive templates, namely PAMAM dendrimers[25], and polylysine.[26] The emission spectrum, on the other hand, shows a pronounced red-shift moving from 644 nm and 704 nm, in water, to 665 nm and 727 nm, in PAH aqueous solution. The measurements with TSPP were performed at pH=7.0 in order to avoid its diacid form. The monoexponential decay yielding a lifetime of 10 ns agree well with other published results [27] and show that TSPP is in its monomeric form. This solution is used as reference for TSPP incorporated in PE microcapsules.

b) Tetra-(4-N-methylpyridyl)porphyrin, TMPyP/PSS

TMPyP is a tetra-cationic porphyrin with a fluorescence quantum yield (ϕ_F) of 0.047 in water.[28] Its absorption spectrum presents the typical bands of free-base porphyrins: a Soret band at 421 nm and four Q bands between 500-700 nm (Fig. S2). The corresponding emission spectrum is unresolved having its maximum at 717 nm. The vibrational structure of TMPyP emission spectrum in water is unresolved due to band broadening, and the Q(0,0) emission band appears as a shoulder relative to the more intense Q(0,1) band. When TMPyP is added to an aqueous solution of the oppositely charged PSS, there are clear evidences of complexation to the polyelectrolyte and also of its aggregation. The Soret absorption is slightly red-shifted, broader and less intense

indicating that non-specific aggregates are formed. The emission spectrum gains some vibrational resolution due to the complexation of the methylpyridinium groups of the porphyrin to the sulfonate groups of the polyelectrolyte. Also, the losses in emission intensity due to TMPyP aggregation seem to be compensated by the porphyrin quantum yield recovery because charge transfer within the TMPyP is no longer possible.

c) 2-[2-(2-methylpyridinium)-vinyl]-5,10,15,20-tetraphenylporphyrin, BOPYP/PSS

BOPYP is a mono-cationic porphyrin that bears a 2-N-methylpyridinium porphyrin covalently linked to a β-vinyl-meso-tetraphenylporphyrin. Its absorption spectra is different from the ones of TMPyP and TSPP and extremely dependent on the solvent`s nature (Fig. S3). In addition to the typical Soret and Q absorption bands of meso-tetrarylporphyrins, the electronic absorption spectra of BOPYP presents a new band (455-505 nm), that was related with the existence of a trans/quinoid structure in the ground state.[29] The emission profile is less complex than the absorption spectra. However, in water, the Q(0,0) and Q(0,1) bands, usually around 660 and 730 nm, are less resolved.

Unlike tetracationic TMPyP and tetraanionic TSPP, BOPYP is sparingly soluble in water. Efforts to decrease porphyrin insolubility where made by using the polyelectrolyte pair, PSS/PAH at different pH values (2.8 and 6.5). Significant spectral changes are observed in PSS solutions at pH 2.8 when compared with the ones obtained in water, as seen by a significant red-shift of the Soret band and a decrease of the number of Q bands. This spectrum is typical of the bis-protonation of the porphyrinic inner core with loss of symmetry and predicts the formation of a fluorescent porphyrin-polyelectrolyte complex that bears the porphyrinic moiety in a tricationic form.

B. Electrostatic adsorption of fluorophores in PAH/PSS microcapsules

Ionic Porphyrins

The incorporation of water soluble ionic porphyrins in microcapsules was studied by steady-state electronic absorption and emission, and by FLIM. Using the LbL technique the best interaction was found between ionic dyes and polyelectrolytes oppositely charged.

The results obtained for the porphyrins in the microcapsules are compared with those obtained in solution: porphyrin free in water and complexed with the oppositely charged polyelectrolyte.

a) *meso*-Tetra (4-sulfonatophenyl) porphyrin, TSPP

The behaviour of TSPP in PE MCs, both inside the shell and at the interface microcapsule-water, is different from that observed in aqueous solutions of PAH. Although PAH works as a vehicle for the incorporation of TSPP in the MCs, electrostatic interactions between the two are somehow broken and porphyrin molecules displaced, in order to allow the polyelectrolyte to interact with the previous layer of PSS in the MC. Also, the PAH chain becomes much more extended to allow the connection through multiple binding sites to the microcapsule, moving away part of the porphyrins and separating them from each other. TSPP encapsulated in microcapsules shows a broad and red-shifted Soret absorption; the emission maximum appears between those observed with the monomer in water and with the aggregates of TSPP in aqueous PAH (Fig. 1).

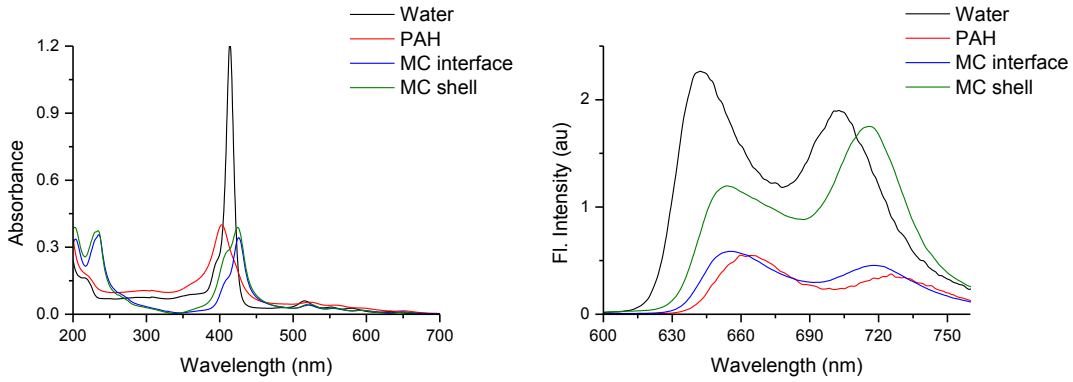

Fig. 1 Absorption and emission spectra of TSPP in different environments. TSPP in solution: [TSPP] = 2 μM; [PAH] = 0.2 μM; λexc = 405 nm. TSPP in microcapsules: λexc = 430 nm.

Table 1 Fluorescence lifetimes of TSPP in aqueous solutions and PE MCs at pH=7.0.

	τ_1 (ns)	A_1 (%)	τ_2 (ns)	A_2 (%)	τ_3 (ns)	A_3 (%)	τ_{avg}	χ^2
Water	10.0	100	-	-	-	-	10.0	1.066
PAH	10.9	38	-	-	1.0	62	9.6	1.187
MC interface	9.8	34	3.7	27	0.8	40	7.9	1.052
MC shell	9.9	40	3.7	32	0.8	29	8.1	1.033

Moreover, the heterogeneous environment around TSPP in microcapsules results in more complex fluorescence decays. These decays were analysed with a multi-exponential function, yielding three discrete lifetimes (Table 1). From the lifetime results it can be concluded that the organization of TSPP in MCs is rather different from that in PAH aqueous solutions. The interpretation of the lifetime results is not so straightforward due to the presence of a 3.7 ns intermediate lifetime, which is identical to the monomeric diacid form of TSPP lifetime. Three representative FLIM images of the microcapsules with TSPP are presented in Fig. 2. It can be inferred from the images that porphyrins are homogeneously distributed in the microcapsules. There is a quite narrow distribution of lifetimes, with the exception of a few regions where shorter average lifetimes are detected (blue pixels). These ones might correspond to microcapsules with higher local pHs or to microcapsules where the porphyrins are more aggregated,[30] as above mentioned. The irregularity in the shape and size of the microcapsules concerns to the template used, which in this case was precipitated calcium carbonate particles.

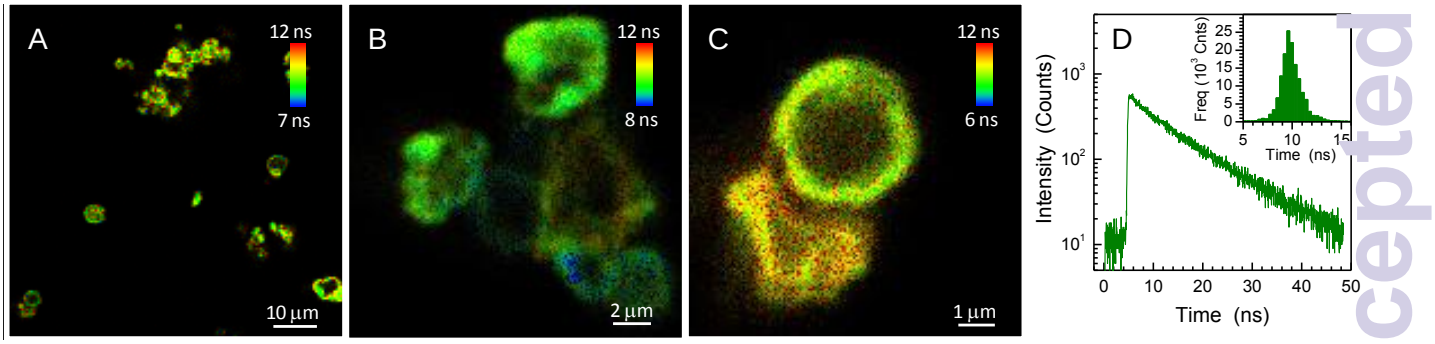

Fig. 2 FLIM images(A,B,C) of polyelectrolyte microcapsules templated on CaCO3 microparticles. The microcapsules contain the following sequence of layers:(PAH/PSS)4-(PAH-TSPP)-PAH/PSS. D) Fluorescence decay and lifetime histogram (inset) from image A.

Fluorescence

b) Tetra-(4-N-methylpyridyl)porphyrin, TMPyP

The absorption spectra of TMPyP in the microcapsules show a narrower and red-shifted Soret band as compared to TMPyP in PSS. The emission bands are observed at 653 nm and 718 nm, respectively, with the vibrational structure of the porphyrin completely recovered (Fig. 3).

Fluorescence decays are well fitted with a bi-exponential function (Table 2). It is worth noticing that each single component is perhaps the average value of a non-homogeneous population but, in any case, the longer and the shorter lifetimes are likely to represent two different populations of monomeric and aggregated porphyrins, respectively. Both lifetime components increase due to the association of porphyrin to PSS, but the two-fold increase in the longer lifetime component is a well documented signature of TMPyP complexation. Interestingly, lifetimes for TMPyP at the MC interface are similar to those obtained with PSS in solution but in the MC wall there is again a quite significant increase in the longer component. The increase in fluorescence quantum yield and lifetime has been widely reported for fluorophores in frozen solutions (reduced thermal agitation) and also for membrane and protein-bonded fluorophores. This phenomenon has been attributed to a decrease in the energy loss by non-radiative deactivation processes (collisions with solvent molecules, intramolecular vibrations and rotations, etc.).

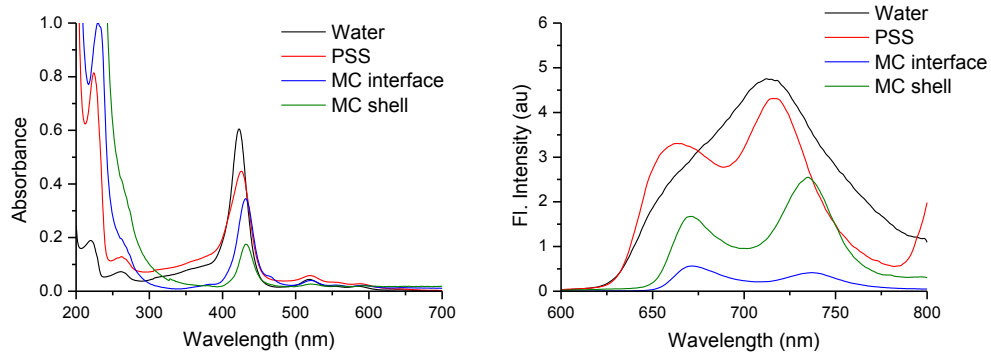

Fig. 3 Absorption and emission spectra of TMPyP in different environments. TMPyP in solution: [TMPyP] = 2μM; [PSS] = 0.2 μM; λexc = 405 nm. TMPyP in MCs: λexc = 430 nm.

Table 2 Fluorescence lifetimes of TMPyP in aqueous solutions pH=5.6 and in PE MCs

	τ_1 (ns)	A_1 (%)	τ_2 (ns)	A_2 (%)	τ_{avg}	χ^2
Water	5.3	89	1.7	11	5.2	1.065
PSS	10.5	62	3.2	38	9.4	1.102
MC interface	10.7	63	5.4	37	9.5	1.075
MC shell	12.8	81	6.0	19	12.1	1.088

In the case of the ionic porphyrins studied (porphyrins bound to MC interface vs. porphyrins inside MC shell), the decrease in the non-radiative decay rates that lead to the simultaneous increase in emission intensity and average lifetime should mainly arise from the restricted rotational freedom of the ion meso-aryl substituents connected to the PE matrix by electrostatic interactions.

FLIM images of these microcapsules are presented in Fig. 4 and they are very similar to the images of the microcapsules with the oppositely charged TSPP. TMPyP seems to be rather homogeneously distributed within these microcapsules.

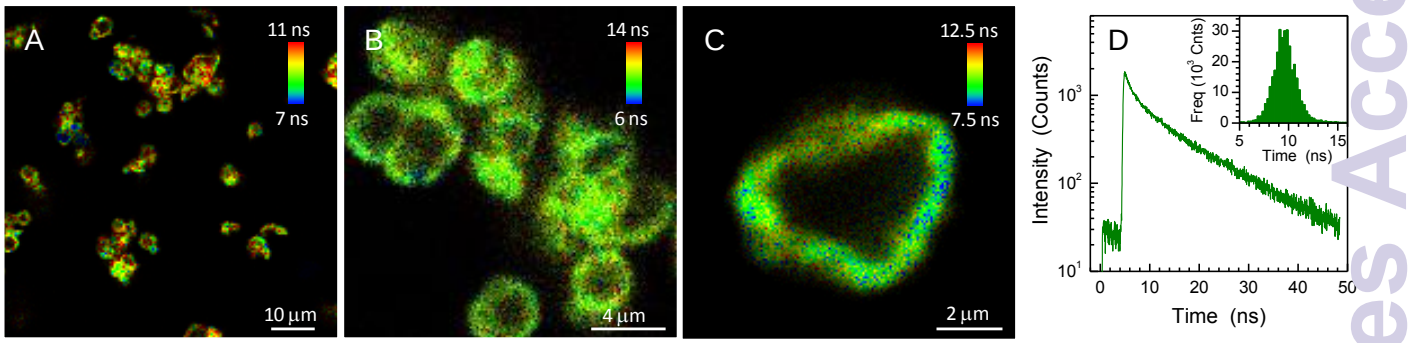

Fig. 4 FLIM images of polyelectrolyte microcapsules templated on $CaCO_3$ microparticles. The microcapsules contain the following sequence of layers: $(PAH/PSS)_4$-PAH-(PSS-TMPyP)-PSS/PAH. D) Fluorescence decay and lifetime histogram (inset) from image A.

Unlike its free base equivalent, ZnTMPyP has no tendency to aggregate in water and remains monomeric upon interaction with the oppositely charged PSS. The absorption and the emission spectra (not shown) indicate a red-shift but no broadening or reduction in absorption. Also, the emission spectrum is not affected by the binding of the porphyrin, with the exception of a few changes in the relative intensities of the Q(0,0) and Q(0,1) bands. Fluorescence decays are mono-exponential with a short-lived component of 1.3 ns in water and 1.4 ns in aqueous PSS, which are consistent with other values reported in literature.[31] In microcapsules, an additional red-shift in the Soret absorption is detected. The decrease in absorption intensity observed going from the MC interface to the MC shell is a consequence of the displacement of a considerable high amount of porphyrin adsorbed to the microcapsules during the binding of the next layer of PAH. The fluorescence decays (Table 3) are now fitted with a bi-exponential decay law, introducing another component which is about half of the longer lifetime. In such a heterogeneous system, as above referred to, these discrete lifetimes might correspond to the average of two distinct porphyrin populations. The longer lifetime may be assigned to the monomer but the assignment of the shorter one is not so straightforward. It might correspond to the average lifetime of a population of porphyrins quenched by the amine groups of PAH in microcapsules. Quenching by electron transfer from PAH is very unlikely since PAH is fully protonated at the pH=5.6 used.

Table 3 Fluorescence lifetimes of ZnTMPyP in aqueous solutions and in PE MCs, at pH=5.6.

	τ_1 (ns)	A_1 (%)	τ_2 (ns)	A_2 (%)	τ_{avg}	χ^2
Water	1.3	100	-	-	1.3	1.137
PSS	1.4	100	-	-	1.4	1.061
MC interface	1.3	55	0.6	45	1.0	1.162
MC shell	1.7	57	0.9	43	1.4	1.038

Once again, it can be noticed a significant increase in the lifetime of the porphyrin when it is deeper inside the MC wall.

FLIM images present the same effect (Fig. 5). The histograms in Fig. 5 C show the distribution of the average lifetimes for each image (A and B). The average lifetimes here are slightly higher than those obtained in the ensemble measurements. Nevertheless, the increase in the maximum of the lifetime distribution going from the interface, (PAH/PSS)4-PAH-(PSS-ZnTMPyP), to the interior of the wall, (PAH/PSS)4-PAH-(PSS-ZnTMPyP)-PSS/PAH, agrees well with the results obtained in solution.

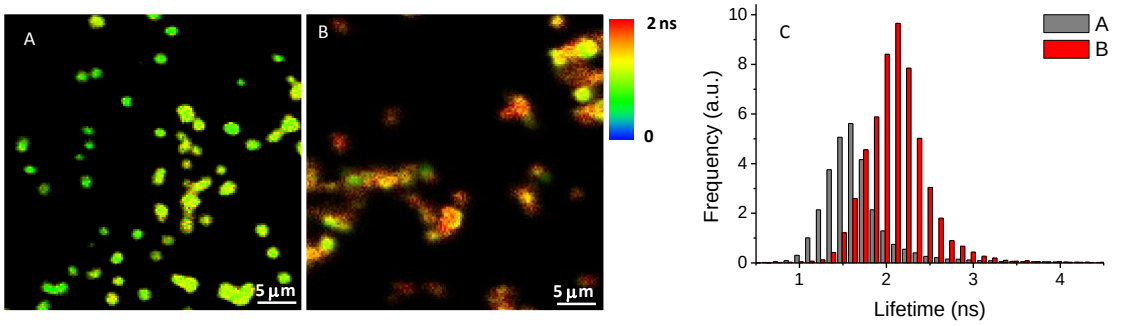

Fig. 5 FLIM images of polyelectrolyte microcapsules templated on MnCO3 microparticles. The microcapsules contain the following sequence of layers: A) $(PAH/PSS)_4$-PAH-(PSS-ZnTMPyP); and B)$(PAH/PSS)_4$-PAH-(PSS-ZnTMPyP)-PSS/PAH. C) Lifetime histogram of images A and B.

c) 2-[2-(2-methylpyridinium)-vinyl]-5,10,15,20 tetraphenylporphyrin, BOPYP

The shape of the emission band obtained in PSS solution (pH 2.8) which is typical of a protonated porphyrin, is preserved in the microcapsule structure. The encapsulation at the MC interface results in a small blue shift in the emission band that is more significant when BOPYP is inside MC shell.

Fluorescence decays are well fitted with a bi-exponential function (Table 4). Similarly to the other pyridinium porphyrins, TMPyP and its zinc complex ZnTMPYP, lifetimes of the longer component BOPYP increase in polyelectrolyte microcapsule shell.

Table 4 Fluorescence lifetimes of BOPYP in polyelectrolyte aqueous solutions and in PE MCs, at pH=2.8 and pH = 6.5.

	τ_1 (ns)	A_1 (%)	τ_2 (ns)	A_2 (%)	τ_{avg}	χ^2
Water	1.3	100	-	-	1.3	1.137
PSS	1.4	100	-	-	1.4	1.061
MC interface	1.3	55	0.6	45	1.0	1.162
MC shell	1.7	57	0.9	43	1.4	1.038

Fig. 6 shows the FLIM images obtained after BOPYP incorporation at MC interface. It is interesting to note that porphyrin distributions depend on the pH of PSS used for MCs preparation. While a uniform distribution around the shell walls was obtained using pH 2.8, BOPYP is randomly oriented in the multi-layered structure at pH 6.5. A decrease in the distribution maxima of fluorescence lifetimes agrees with the differences accounted. The main advantage of using pH 6.5 is to assure the proper ratio of free amine (PAH) and free sulphonate groups (PSS) which controls the layer by layer adsorption of the polyelectrolytes through electrostatic interactions, assuring shell growth and stability.

The nature of the polyelectrolyte and also the encapsulation procedure strongly influences BOPYP's distribution in polyelectrolyte microcapsules. When replacing the strong PE (PSS) by a weak PE polyacrylic acid (PAA) at pH 6.5, significant different FLIM images are obtained. Direct addition of the porphyrin to a PAA/PAH microcapsule also results in uniform distributions around the shell walls. Unexpectedly, well defined circular shapes can be found in the polyelectrolyte or MC shells when BOPYP was assembled simultaneously with PAA (Fig. S4).

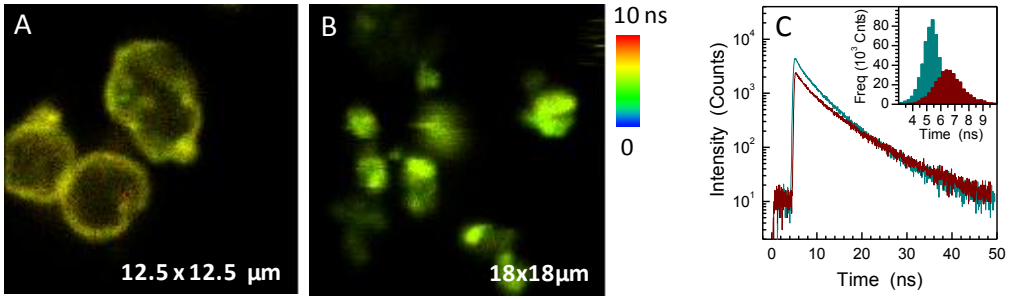

Fig. 6 FLIM images of polyelectrolyte microcapsules doped with BOPYP [(PAH/PSS)5-BOPYP] at different pH values (A) pH 2.8, (B) pH 6.5. D) Fluorescence decay and lifetime histogram (inset) from images A (dark red) and B (dark cyan).

B2. PAH/PSS microcapsules carrying a tetra-carboxylated porphyrin

Microcapsules with tetra-carboxyphenyl porphyrin covalently linked to PAH

Another way to incorporate fluorophores inside polyelectrolyte microcapsules is by the LbL assembly of one or more layers of a polyelectrolyte labeled covalently with the fluorophore. However, this strategy is limited as to whether it is possible to couple the desired fluorophore to a specific polyelectrolyte, which depends on the existence of suitable groups for functionalization, in both molecules. The great advantage of this method is that less fluorophore molecules are removed from the capsules during the further PE adsorption and washing, thus leading to a higher amount of fluorophore encapsulated. Moreover, the linkage can be easily achieved if the polyelectrolyte has primary amine groups and the fluorophore has carboxylate groups, or vice versa. In this case, attaching both molecules by a covalent bond requires only a simple amide coupling reaction.

Since the positive polyelectrolyte (PAH) used in this work had already a high density of primary amine groups, the obvious choice was to find a fluorophore with carboxylic groups. Therefore, a tetra-substituted porphyrin (TCPP) was selected, taking advantage of the pKa of their carboxylic groups. TCPP is interesting because it has a transition from low to high solubility in water at pH values above its pKa=5.8,[17] when the carboxyl groups become deprotonated. A water-soluble carbodiimide, 1-Ethyl-3-(3-dimethylaminopropyl)carbodiimide (EDC), and N-hydroxysuccinimide (NHS) were used to label PAH with TCPP (Fig. S5).

The pH chosen for adsorption of TCPP-PAH onto the microcapsules is extremely important. This adsorption is controlled by the free amine groups of PAH, which are in large excess since the labelling reaction was performed with a molar ratio TCPP/PAH of 1:1. Regarding this, the non-purified reaction mixture can be added to the microcapsules to assemble TCPP-labelled PAH, at a convenient pH that avoids the adsorption of other molecules present in the reactional mixture to the MC. This step was performed at pH 5.6 because it assures that the PAH is fully protonated and the other molecules are neutral, being thus removed through the subsequent centrifugation/washing steps.

In water, at a pH where carboxylic acid groups of TCPP are ionized, the maximum of Soret band appears at 414 nm.[19] In PE MCs, at pH=7, the Soret maximum is observed at the same wavelength (Fig. S6) and Qx(0,0) and Qy(0,1) are observed at 647 nm and 706 nm, respectively. These values are very close to those reported for the covalent linked TCPP-silsesquioxane in periodic mesoporous organosilicas (PMOs).[32]

At pH=7, most of the carboxylic groups of TCPP are dissociated. PAH has a pKa of about 8.6 in solution, which might be actually higher in polyelectrolyte multilayers,[19] and so it is likely to be fully protonated. Thus, a shift in pH from 5.6 to 7 is expected to induce the coupling of carboxylate porphyrin with the free charged amines of PAH in the microcapsule. This was verified by FLIM, with the time-resolved images (Fig. S7A,B) and also with the decays obtained from several points in the acquired images. The data treatment yielded the histograms with the average lifetimes in Fig. 7C, and the tri-exponential decay analysis represented on Table 5.

Table 5 Fluorescence lifetime decays of the microcapsules with TCPP-labelled PAH Several points from FLIM images were analyzed and the average results are presented.

	τ_1 (ns)	A_1 (%)	τ_2 (ns)	A_2 (%)	τ_3 (ns)	A_3 (%)	τ_{avg}	χ^2
pH 5.6	10.1	79	3.6	17	0.5	4	8.7	1.052
pH 7.0	11.2	86	4.2	11	0.6	3	10.1	1.041

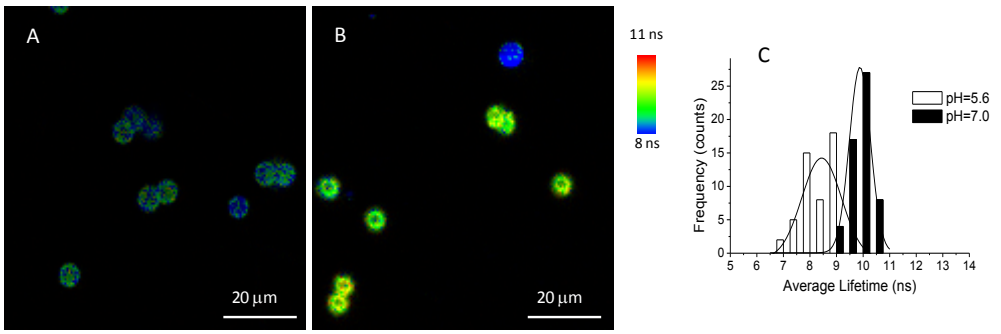

Fig. 7 Microcapsules of TCPP-PAH at pH=5.6 (A) and at a pH between PAH and TCPP pKa's (pH=7.0) (B). Excitation was performed at 405 nm. (C) Histograms of the average lifetime of TCPP-PAH microcapsules at pH 5.6 (hollow bars) and pH 7 (filled bars). The histograms were fitted with Gaussian functions.

A small shift of the suspension pH (from 5.6 to 7) produces a significant increase in the average lifetime of the porphyrin inside the microcapsule wall (8.7 to 10.1 ns). Moreover, this increase in pH results in a narrower distribution of the average lifetime, τ_{avg}. So, as we have anticipated, the ionization of the carboxylic groups in PAH-TCPP improves the interaction with the oppositely charged PAH thus leading to an increase in the fraction of porphyrin long-lived monomers in PAH/PSS microcapsules.

The increase in pH 5.6 to pH 7.0 also resulted in a delocalization of the maximum intensity towards a more internal region of the microcapsule (Fig. 8). This is quite unexpected since, as mentioned before, the increase in the pH is expected to result in the swelling of the PAH/PSS multilayers. In fact, swelling would only be expected at pH values well above pH=7.0. Therefore, this feature on FLIM images is not a result of charge equilibria controlled by the PAH ionization degree, which is almost unaffected, but rather it must be controlled by the ionization of porphyrin carboxylic groups. The composition of microcapsules is (PAH/PSS)5-(PAH-TCPP)-PSS.

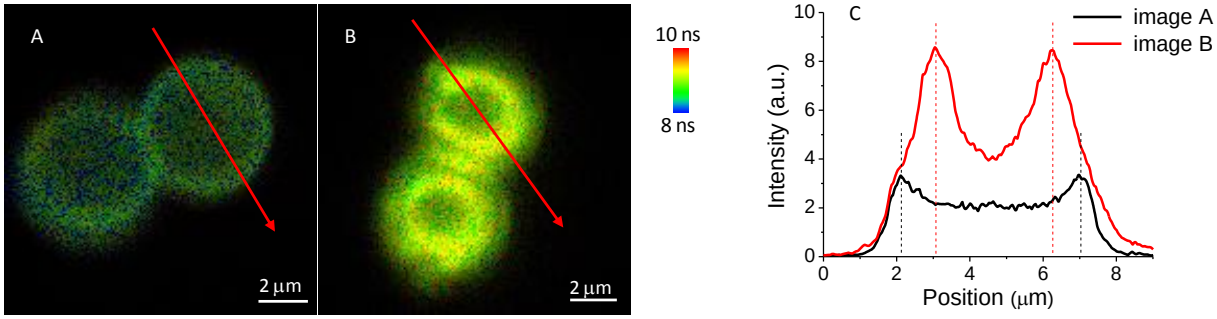

Fig. 8 Microcapsules with the sequence $(PAH/PSS)_5$-(PAH-TCPP)-PSS in water at: (A) pH=5.6; and (B) pH=7.0. (C) Intensity profiles of the red arrows in images A and B.

As TCPP becomes more ionized, the porphyrin tends to be more monomeric and to establish more electrostatic interactions with PAH. Porphyrin carboxylates will have to interact with more internal PAH groups, since there are no PAH layers after the PAH-TCPP layer. This might be the reason for the effect observed in FLIM images.

B3. PAH/PSS microcapsules carrying phthalocyanines

a) Tetrasulfonated aluminum phthalocyanine, $AlPcS_4$

Here, we focus on the FLIM results (Fig. S7) that show that $AlPcS_4$, contrasting with previous reports,[33] adsorbs to the MCs as a monomer, exhibiting a lifetime of 4.9 ns. This lifetime is identical to the one reported in literature for the same phthalocyanine complexed with PAMAM dendrimers at a pH where amine groups are protonated.[34] The lifetime histogram shows a quite narrow distribution, as it would be expected for homogeneous environments with monomeric fluorophores. It is worth noticing that the adsorption of the phthalocyanine to the microcapsule in its monomeric form was only possible because we used a $AlPcS_4$ dipping solution with a concentration of 10^{-7} M, which is about 1000x more diluted than the typical concentration used with porphyrins. Here commercial polymeric particles were chosen as templates in the preparation of microcapsules. By using these templates, microcapsules are produced with a very narrow size distribution but the polymeric cores are extremely difficult t

remove and, thus, scattering artifacts are usually very pronounced with these microcapsules.

b) Monosulfonated aluminium phthalocyanine entrapped within the lipid bilayer coating of microcapsules

Addition of DMPC vesicles to polyelectrolyte MCs is expected to result in the adsorption of a single bilayer of lipid covering the entire surface of the microcapsules. This can be very useful to assemble hydrophobic fluorophores onto microcapsules. Since the fluorophore is in a lipophilic environment, aggregation is unlikely to occur. Thus, the fluorophore is able to preserve its photophysical properties. Another important aspect is that fluorophores might not be as randomly oriented as when they are directly linked to the microcapsule.

On the other hand, the interaction of the fluorophores inside the lipid bilayer with any molecule in the microcapsule shell is limited by a distance threshold that can reach a few nanometers (lipid bilayer thickness is approximately 5 nm).

Here, $AlPcS_1$ was incorporated in DMPC vesicles before coating the microcapsules with the lipid bilayer, which was performed at a temperature above the Tm of the lipid. If a single bilayer of lipid is formed around the microcapsule surface, the intensity will be homogeneously distributed in the intensity image of that microcapsule. FLIM images of lipid-coated PAH/PSS microcapsules templated on $CaCO_3$ are presented on Fig. 9. The fluorescence decays of $AlPcS_1$ in lipid-coated microcapsules are now, as expected, mono-exponential and identical to those observed in vesicles' suspensions (τ_{avg} = 5.0 ns). Moreover, the narrow distribution of the average lifetimes reflects a more homogeneous environment (Fig. 9).

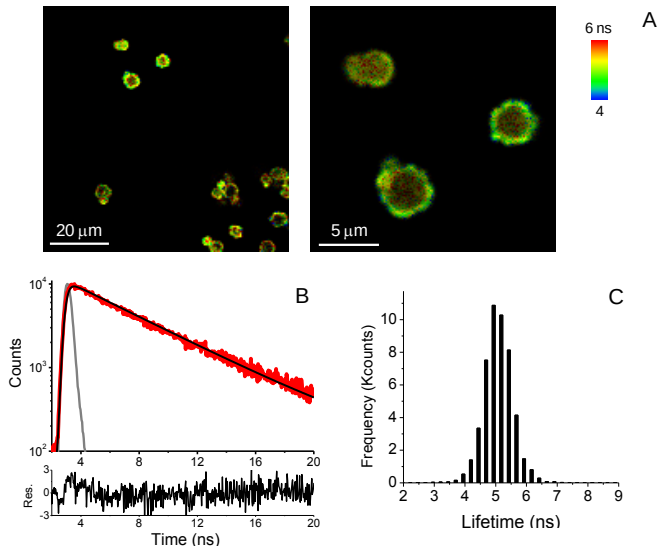

Fig. 9 (A) Lifetime image of DMPC lipid-coated microcapsules (left) and zoom of the same image (right); (B) Lifetime decay of the left image in (A), fitted by a single-exponential decay time of 5 ns; and (C) Lifetime histogram of the same image. The template used was $CaCO_3$ microparticles; $AlPcS_1$ was incorporated in DMPC vesicles before the lipid-coating of MCs.

C. Interaction of phthalocyanines with gold nanoparticles in polyelectrolyte microcapsules

Absorption and emission spectra of mono- and tetrasulfonated phthalocyanines ($AlPcS_1$ and $AlPcS_4$) superimposes onto the red-edge of the surface plasmon resonance absorption of AuNPs. Since plasmon-enhanced fluorescence emission of $AlPcS_4$ in PE films[35] was already observed we could expect that it would also be possible to detect it in PEs MCs.

C1. AuNPs/$AlPcS_4$

We prepared these novel systems with phthalocyanine using, once again, the $CaCO_3$ as template. Attempts to increase fluorophore-metal interactions by increasing the amount of AuNPs adsorbed to the MCs were made by a second addition of AuNPs, after another layer of PAH. These microcapsules were prepared according to the following schemes:

A) control: $(PAH/PSS)_6$-PAH-$AlPcS_4$;

B) sample: $(PAH/PSS)_4$-PAH-AuNPs-PAH-AuNPs-$(PAH/PSS)_4$-PAH-$AlPcS_4$.

The plasmon absorption band of AuNPs whose average diameter was of 21 nm (determined from TEM images) partially overlaps in the red region with the absorption and emission of $AlPcS_4$ (Fig. S8)

Fig. 10 shows two FLIM images of $AlPcS_4$ microcapsules with and without AuNPs, and the corresponding fluorescence lifetime decays. Although no effect of the nanoparticles on the phthalocyanine emission lifetime has been observed in ensemble measurements (data no shown), some local effects were detected by FLIM. With the lifetime scale employed in the images (2-5 ns), it can be seen that there are blue rounded features that might correspond to regions of the microcapsule where fluorophore-nanoparticle plasmonic interactions take place. Since these confined spots have dimensions close to o[illegible] resolution limit, they might effectively correspond to interactions that occur at a nanometric scale, between a rather small fraction of nanoparticles and fluorophores.

We might also hypothesize that these spots correspond to an increased local aggregation of the phthalocyanine but, should this be the case, the aggregation of phthalocyanine would have been caused by the introduction of nanoparticles in microcapsules. Since the nanoparticles are expected to increase the surface area of the microcapsules,[36] the local aggregation of phthalocyanine due to the nanoparticles is unlikely to occur.

C2. AuNPs/$AlPcS_1$@lipid bilayer

As discussed before, when the phthalocyanine is introduced in microcapsules inside the lipid bilayer no aggregation occurs. Here, we took advantage of that effect to study th[illegible] interactions of gold nanoparticles and phthalocyanines in microcapsules. So, the previous set of microcapsules was repeated, but now with the electrostatic adsorption of a lip[illegible] bilayer with $AlPcS_1$ instead of the free $AlPcS_4$. Thes[illegible] microcapsules were prepared according to the followin[illegible] schemes:

A) control: $(PAH/PSS)_6$-PAH-$AlPcS_1$@lipid BL
B) sample: $(PAH/PSS)_4$-PAH-AuNPs-PAH-AuNPs-$(PAH/PSS)_4$-PAH-$AlPcS_1$@lipid BL.
A few representative FLIM images of these microcapsules A) and B) are presented in Fig. 11. Also some intensity profiles selected with arrows 1, 2, 3 in image C and the lifetime decays obtained from A and C, respectively, are presented. It is confirmed that the lifetime decays obtained with the microcapsules without AuNPs are mono-exponential, and that the corresponding lifetime, of 4.9 ns, can be safely assigned to the monomeric phthalocyanine. Once again, the effect of AuNPs is heterogeneously distributed over the different microcapsules within a same sample and, also, over different regions within the same microcapsule (Fig. 11 C-E). The influence of gold in the fluorescence emission is slightly more pronounced when the phthalocyanine is added within the lipid bilayer coating the MCs; but still, the effect is very localized and heterogeneous. Furthermore, there are regions where the emission intensity seems to be lowered and other regions where it looks brighter. These microcapsules are optically very heterogeneous and the differences in intensity are probably a consequence of both quenching and enhancement effects, occurring simultaneously in different regions of the microcapsules (Fig. 11).
From a global analysis of the results, it is difficult to assume that these microcapsules incorporating metal nanoparticles and fluorophores are suitable to produce plasmon enhanced fluorescence. This should be mainly caused by an insufficient density of nanoparticles in the microcapsules, which leads to a low probability for the occurrence of fluorophore-nanoparticle interactions.

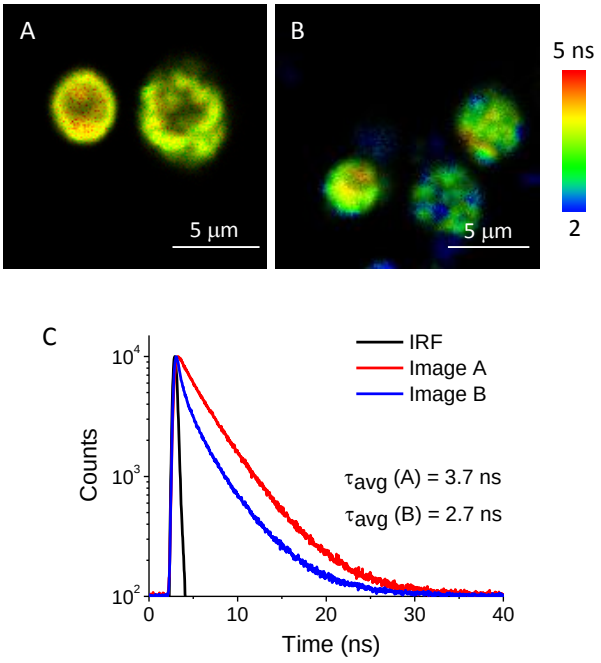

Fig. 10 FLIM images of (A) $(PAH/PSS)_6$-PAH-$AlPcS_4$ microcapsules (control); and (B) $(PAH/PSS)_4$-PAH-AuNPs-PAH-AuNPs-$(PAH/PSS)_4$-PAH-$AlPcS_4$ microcapsules. (C) Fluorescence decays obtained from images A and B.

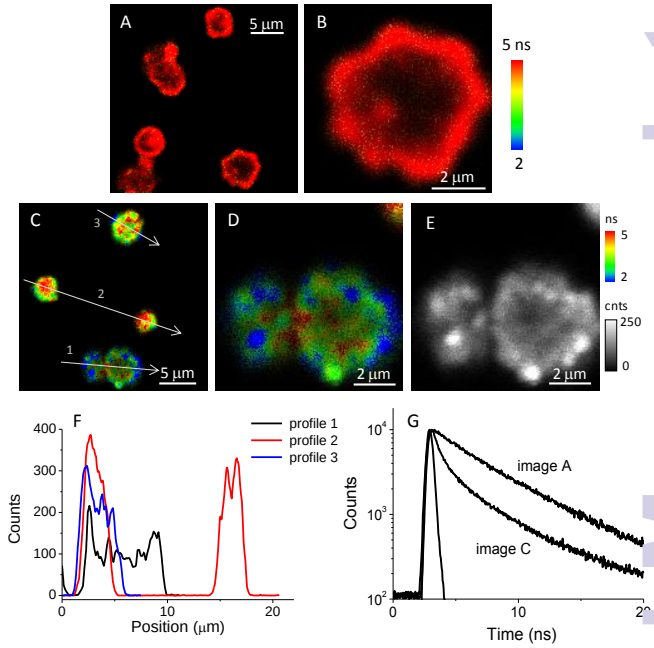

Fig. 11 FLIM images of the microcapsules with (A, B) $(PAH/PSS)_6$-PAH-$AlPcS_1$@lipid BL; and (C, D) $(PAH/PSS)_4$-PAH-AuNPs-PAH-AuNPs-$(PAH/PSS)_4$-PAH-($AlPcS_1$@lipid bilayer) (B) and (D) are zooms of A and C, respectively. (E) Image D - intensity scale. (F) Intensity profiles from images in C. (G) Fluorescence decays obtained from the images A and C.

In order to control the emission enhancements a modified system was designed. A gold nanoparticle was incorporated into a core-polyelectrolyte–shell assembly with a coating lipid vesicle encapsulating the same phthalocyanine dye, $AlPcS_1$. Interestingly, large fluorescence enhancements were obtained, up to three orders of magnitude.[37] Here, the fluorophore-nanoparticle interactions were more effective in hot-spots created by the clustering of gold nanoparticles throughout the LbL polyelectrolyte deposition.

Conclusions

Polyelectrolyte microcapsules work as special scaffolds that hold porphyrinoids either at the interface or in the microcapsule shell restricting the molecules in a confined space. Electrostatic adsorption of charged porphyrins and phthalocyanines, to the microcapsules, is a fairly random process, by which molecules have to diffuse to meet a non-compensated opposite charge of the last adsorbed polyelectrolyte. One limitation of these fully self-assembled systems is the small amount of adsorbed fluorophores remaining in the microcapsule after the process is completed, even with multi-charged fluorophores as TSPP or TMPyP. The covalent approach achieved with TCPP-PAH, is more effective to incorporate larger amounts of fluorophores. On the other hand, the inclusion of a phthalocyanine in a lipid vesicle allows a better separation from nanoparticles dispersed in the aqueous solution inside the microcapsule. Although the modified microcapsules were successfully produced a very small evidence of metal enhanced fluorescence was detected. Fluorescence lifetime contrast-based imaging provides new insights in the field of polyelectrolyte microcapsules.

Acknowledgements

Authors gratefully acknowledge financial support from Fundação para a Ciência e a Tecnologia for finantial support through Projects REEQ/115/QUI/2005, FCT(Pest-OE/QUI/UI0100/2011 and FCT (Pest-OE/QUI/UI0100/2013/2014. Thanks are also due to E.M.P.S and Prof. Maria G.P.M.S Neves for a kind gift of sample BOPYP. R.T. acknowledges a Ph.D. grant SFRH/BD/39006/2007 and VVS a SFRH/BPD/7420/2010. S.A. and P.M.R.P. acknowledge Research Grants from FCT (Program Ciência 2007 and 2008).

Notes and references

1 E. Donath, G. B. Sukhorukov, F. Caruso, S. A. Davis and H. Möhwald, *Angew. Chem. Int. Ed.*, 1998, **37**, 2202.
2 F. Caruso, R. A. Caruso and H. Möwald, *Science*, 1998, **282**, 1111.
3 F. Caruso, H. Lichtenfeld, M. Giersig and H. Möhwald, *J. Am. Chem. Soc.* 1998, **120**, 8523.
4 A. G. Skirtach, A. M. Yashchenok and H. Möhwald, *Chem. Commun.*, 2011, **47**, 12736.
5 V. Gribova, R. Auzely-Velty and C. Picart, *Chem. Mater.*, 2012, **24**, 854.
6 J. Zhang, R. J. Coulston, S.T. Jones, J. Geng, O. A. Schermanand and C. Abell, *Science*, 2012, **335**, 690.
7 B. S. Kim and J.W. Choi, Biotechnol. *Bioprocess. Eng.*, 2007, **12**, 323.
8 C. S. Peyratout and L. Dähne, *Angew. Chem. Int. Ed.*, 2004, **43**, 3762.
9 D. L. Roberts, Y. Ma, S. E. Bowles, C. M. Janczak, J. Pyun, S. S. Saavedra and C. A. Aspinwall, *Langmuir*, 2009, **25**, 1908.
10 M. F. Bédard, B .G. De Geest, A.G. Skirtarch, H. Möhwald and G. B. Sukhorukov, *Adv. Colloid Interface Sci.*, 2010, **158**, 2.
11 M. F. Bedard, S. Sadasivan, G. B. Sukhorukov and A. Skirtach, *J. Mater. Chem.*, 2009, **19**, 2226.
12 K. Suhling, P. M. W. French and D. Phillips, *Photochem. Photobiol. Sci.*, 2005, **4**, 13.
13 R. Teixeira, S. M. Andrade, V. Vaz Serra, P. M. R. Paulo, A. Sánchez-Coronilla, M.G. P. M. S. Neves, J. A. S. Cavaleiro and S. M. B. Costa, *J. Phys. Chem. B*, 2012, **116**, 2396.
14 B. Stadler, R. Chandrawati, K. Goldie and F. Caruso, *Langmuir*, 2009, **25**, 6725.
15 S. Nizamoglu, M. C. Gather and S. H. Yun *Adv. Mater*. 2013, **25**, 5943.
16 M. Schubert, A. Steude, P. Liehm, N. M. Kronenberg, M. Karl, E. C. Campbell, S. J. Powis and M. C. Gather *Nano Lett.* 2015, **15**, 5647.
17 R. Chandrawati, P. D. Odermatt, S. Chong, A. D. Price, B. Städler and F. Caruso, *Nano Lett.*, 2011, **11**, 4958.
18 M. Ambroz, A. Beeby, A. J. MacRobert, M. S. C. Simpson, R.K Svensen and D. Phillips, *J. Photochem. Photobiol. B*, 1991, **9**, 87-95
19 M. Y. Choi, J. A. Pollard, M. A. Webb and J. L. McHale, *J. Am. Chem. Soc.*, 2003, **125**, 810.
20 E. M. P. Silva, F. Giuntini, M. A. F Faustino, J. P. C. Tomé, M. G. P. M. S. Neves, A. C Tomé, A. M. S. Silva, M. G. Santana-Marques, A. J Ferrer-Correia and J. A. S. Cavaleiro, *Bioorg. Med. Chem. Lett.*, 2005, **15**, 3333.
21 T.-L. Chang, Y.-W. Lee, C.-C. Chen and F.-H. Ko, *Microelectron. Eng.*, 2007, **84**, 1698.
22 J. Rodríguez-Fernández, J. Pérez-Juste, F. J. García de Abajo and L. M. Liz-Marzán, *Langmuir*, 2006, **22**, 7007.
23 M. A. R. B. Castanho, N. C. Santos, L. M. S. Loura, *Eur. Biophys. J.*, 1997, **26**, 253.
24 N. C Maiti, S. Mazumdar and N. Periasamy, *J. Phys. Chem. B*, 1998, **102**, 1528.
25 P. M. R. Paulo and S. M. B. Costa, *Photochem. Photobiol. Sci.*, 2003, **2**, 597
26 L. Zhang and M. Liu, *J. Phys. Chem. B*, 2009, **113**, 14015.
27 S. M. Andrade and S. M. B. Costa, *Biophys. J.*, 2002, **82**, 1607.
28 P. M. R Paulo and S. M. B Costa, *J. Phys. Chem. B*, 2005, **109**, 13928.
29 V. V. Serra, S. M. Andrade, E. M. P. Silva, A. M.S. Silva, M. G. P. M. S Neves and S. M. B. Costa, *J. Phys. Chem. B*, 2013, **117**, 15023.
30 S. M. Andrade and S. M. B. Costa, *Chem. Eur. J.*, 2006, **12**, 1046.
31 P. M. R. Paulo and S. M. B. Costa, *J. Photochem. Photobiol. A*, 2012, **234**, 66.
32 E.-Y. Jeong, A. Burri, S.-Y. Lee and S.-E. Park, *J. Mater. Chem.*, 2010, **20**, 10869.
33 Y. Zeng, X-L. Wang, Y-J Yang, J.-F. Chen, J. Fu and X. Ta *Polymer*, 2011, **52**, 1766.
34 P. M. R. Paulo and S. M. B. Costa, *J. Phys. Chem. C*, 2010, **11** 19035.
35 R. Teixeira, P. M. R. Paulo, A. S. Viana and S. M. B. Costa, *Phys. Chem. C*, 2011, **115**, 24674.
36 A. Dorris, S. Rucareanu, L. Reven, C. J. Barret and R. B. Lennox, *Langmuir*, 2008, **24**, 2532.
37 R. Teixeira, P. M. R. Paulo, S. M. B. Costa, *J. Phys. Chem. C*, 2015, DOI: 10.1021/acs.jpcc.5b04667.

